www.elsevier.com/locate/memsci

Binary iron cobalt oxide silica membrane for Gas separation

Adi Darmawan, Julius Motuzas, Simon Smart, Anne Julbe, João C Diniz da Costa

PII: S0376-7388(14)00735-2
DOI: http://dx.doi.org/10.1016/j.memsci.2014.09.033
Reference: MEMSCI13205

To appear in: *Journal of Membrane Science*

Received date: 14 April 2014
Revised date: 17 September 2014
Accepted date: 18 September 2014

Cite this article as: Adi Darmawan, Julius Motuzas, Simon Smart, Anne Julbe, João C Diniz da Costa, Binary iron cobalt oxide silica membrane for Gas separation, *Journal of Membrane Science,* http://dx.doi.org/10.1016/j.memsci.2014.09.033

Binary Iron Cobalt Oxide Silica Membrane for Gas Separation

Adi Darmawan[1,2], Julius Motuzas[1], Simon Smart[1], Anne Julbe[3], João C. Diniz da Costa[1]*

[1]The University of Queensland, FIMLab – Films and Inorganic Membrane Laboratory, School of Chemical Engineering, Brisbane Qld 4072, Australia.

[2]Diponegoro University, Department of Chemistry, Faculty of Science and Mathematics, Jl. Prof. Soedharto Tembalang, Semarang 50275, Indonesia.

[3]Institut Européen des Membranes, UMR 5635 CNRS, ENSCM, UM2, Université Montpellier 2, Place Eugene Bataillon, 34095 Montpellier cedex 5- France

*corresponding author: j.dacosta@uq.edu.au Tel.:+61 7 3365 6960 Fax: +61 7 3365 4199

Abstract

This work investigates the preparation, characterisation and performance of binary iron/cobalt oxide silica membranes by sol-gel synthesis using tetraethyl orthosilicate as the silica precursor, and cobalt and iron nitrates. It was found that cobalt and iron oxides were generally dispersed homogeneously in the silica structure, with the exception of a few minor patches rich in cobalt oxide. The sol-gel synthesis affected the micro-structural formation of binary metal oxide silica matrices. Increasing the iron content favoured condensation reactions and the formation of siloxane bridges, and consequently larger average pore sizes which lead to low He/N_2 permselectivity values below 20. In the case of high cobalt content, a higher silanol to siloxane ratio was observed with tighter pore size tailoring, as evidenced by higher He/N_2 permselectivities reaching 170. The binary metal oxide and silica interfaces proved to follow a molecular sieving mechanism characterised by activated transport where the permeance of the smaller gas molecules (He and H_2) increased with temperature up to 500 °C, whilst the permeance of larger gas molecules (CO_2 and N_2) decreased.

Key words: iron oxide; cobalt oxide; binary metal oxide doping; silica membranes.

1 Introduction

The sol-gel method is a very versatile technique generally employed to prepare high quality silica derived membranes for gas separation at high temperatures. Embedding metal oxides into silica membranes generally does not affect the micro structural pore formation thus conferring good gas permeation and separation performance. The preferred choices for doping silica matrices include oxides of nickel [1, 2], cobalt [3] and palladium [4], in addition to zirconia [5-7], titania [8], niobia [9, 10] and alumina [11, 12]. Adding metal oxides also provide functionalities to the membranes which otherwise are not available with pure silica.

Examples of functionalities include superior stability under steam exposure of cobalt oxides silica membranes using tetraethyl orthosilicate (TEOS) as the silica precursor [13]. Battersby et al. [14] reported that cobalt silica matrices remained microporous in wet gas streams, whilst pure silica xerogels were greatly affected by closing small pores and opening large pores leading to mesoporous structures. In some cases, the metal oxide can aid the transport of gases by changing adsorption properties for gases such as H_2 for nickel oxide silica amorphous materials [15-16]. In other cases, the oxidation state of cobalt oxide in silica xerogels can be modulated by adding cationic surfactants [17]. In another example, Miller et al. [18] recently reported the unusual effect of reversible redox effect on gas permeation of cobalt oxide doped on ethoxy polysiloxane (ES40) silica precursor.

Another important functionality of metal oxides is the pore size control and stability to other substances. For instance, Uhlmann et al. [19] exposed cobalt oxide silica membranes to H_2S and found that sulfur did not react with cobalt oxide, thus clearly indicating that the silica and cobalt oxide interface had pore sizes below the kinetic diameter of H_2S (d_k=3.6Å). The stability of cobalt

oxide silica membranes were also proven for 2000 hours under thermal cycling tests up to 500 ^{o}C for a scaled-up module containing 8 membrane tubes [20]. In addition, cobalt oxide silica membranes showed excellent performance for the H_2 separation even at higher temperatures of 600 °C [21], a temperature which would lead to thin film densification in the case of pure silica membranes. Very recently, it was proven for the first time that cobalt oxide silica are robust in the preparation of membranes via rapid thermal processing [22, 23], where membranes were manufactured in a single day instead of the conventional slow thermal processing of up to 10-14 days.

The structural tailorability of cobalt oxides makes them the preferred metal oxide doping material in silica membranes. Nevertheless, Darmawan and co-workers [24] recently incorporated iron oxide into silica matrices, producing microporous materials. Iron nitrate has a good solubility, adequate for applying in the sol–gel method [25], leading to the formation of γ-Fe_2O_3 (magnetite) in the silica matrix [26]. Iron oxides also showed excellent dispersion with small particle sizes [27], which tend to confer stronger oxide and matrix interactions [28]. On this basis, the reported properties of iron oxide should justify its potential as a dope material embedded in silica matrices. However, there is a serious mismatch between the coefficient of thermal expansion between silica and iron oxides [29], which is concerning as thin silica films containing iron oxides may crack, thus rendering membranes ineffective.

To address this problem, this work pursues a strategy of binary metal oxide doping by investigating the effect of binary iron and cobalt oxides into silica membranes. Currently there is only a single publication into binary metal oxide doping using cobalt and palladium silica membranes [30]. Palladium is an expensive noble metal, and its replacement with the abundant and cost effective iron oxide is desirable in economic terms. Therefore, this work investigates the physicochemical properties of bulk xerogels prepared via the sol-gel method and containing varying ratios of iron to

cobalt oxides. In addition, the silica membrane performance with varying Fe/Co ratios are tested for single gas permeation for helium, hydrogen, carbon dioxide and nitrogen at temperatures ranging from 200 to 500 °C.

2 Experimental

2.1 Sol-gel synthesis and characterisation

The metal to silicon ratio chosen in this investigation is 1:4 (25 mol%), which is in the range for the best microporous structures as reported by Yacou and co-workers [20] for cobalt oxide silica matrices. A series of samples were prepared by changing the Fe/Co oxide ratio, though the total metal to silicon ratio was kept constant at 1:4. Briefly, Fe/Co oxide sols were synthesised by the hydrolysis and condensation of tetraethyl orthosilicate (TEOS) in ethanol and 30% aqueous H_2O_2 with iron nitrate nonahydrate ($Fe(NO_3)_3.9H_2O$) and cobalt nitrate hexahydrate ($Co(NO_3)_2.6H_2O$). An initial molar ratio of 255 EtOH: 4 TEOS: 1 Metal Nitrate Hydrate: $9H_2O_2$: $40H_2O$ was mixed and vigorously stirred for 3 hours in an ice-cooled bath. The molar concentration of the iron and cobalt (x:y) was varied between 0:1 (0/100) and 1:0 (100/0). Hence, the total concentration of the two metals was always 1 mol in the sol. Blank samples of iron oxide silica (x=1 and y=0) and cobalt oxide silica (x=0 and y=1) were prepared for comparison purposes with the binary metal doped silica structures. Sol samples were dried in a temperature controlled oven at 60 °C and atmospheric conditions to form xerogels. The xerogel samples were crushed finely and calcined at ramp rates of 1.5°C min^{-1} to 600 °C in air atmosphere with a 2.5 hour holding time at the desired temperature.

Nitrogen adsorption was studied at 77 K using a Micromeritics Tristar 3020 to determine the BET surface area and pore volume. The samples were initially degassed for 24 h to pressures of ~2Pa at 200°C. Fourier transform infrared analysis (FTIR) was carried out on a Shimadzu IRAffinity-1 with a Pike MIRacle ATR attachment. Spectra in the relevant regions of silica and metal oxides were taken over a wavelength range of 1300-580cm^{-1}. Scanning electron microscopy (SEM) images of

platinum coated samples were obtained with a JSM-7001F field emission microscope operated at an accelerating voltage of 10 kV with a Si(Li) energy dispersive X-ray spectrometer. The EDX spectra were acquired using an EX-64175-JMH EDX system at 20 kV and 10mm distance. The EDX spectra were analysed with an Integrated JEOL Analyses Station Software (version 3.8).

2.2 Membrane Preparation and Testing

Iron cobalt oxide silica thin film layers were coated on ceramic tubular supports 10 cm in length and 1.4 cm external diameter provided by the Energy Centre of the Netherlands (ECN). These supports have high quality γ-alumina interlayers with an intrinsic pore size distribution centered ~ 4nm, with a very low defect density above 10nm [21, 31], which were coated on α-alumina substrates. The tubular supports were dip-coated with the binary iron cobalt oxide silica sol using a controlled immersion time of 1 min, and immersion/withdrawal speed of 10 cm min^{-1}. Each layer was calcined at 600 ^{o}C in air, and held for 2.5 h with a heating and cooling rate of 1^{o}C min^{-1}. A total of 4 layers were coated onto the alumina support.

The performance of iron cobalt oxide silica membranes was measured by single gas permeation using a custom-made setup (Fig. 1) with a membrane housing module. The temperature of the module was controlled by a furnace with an external PID temperature controller. The membrane tube was sealed using graphite ferrules and stainless steel pressure fitting before being placed inside the module. The single gas permeation was carried out in dead-end mode, where the retentate line was closed and the permeate line was open to atmospheric pressure. The feed pressure of gases in the membrane module was measured by a pressure gauge.

The membrane was then heated and tested for single gas permeance with helium (He), hydrogen (H_2), nitrogen (N_2) and carbon dioxide (CO_2) at decreasing temperatures ranging from 500 °C to 100°C at 50 °C increments with a trans-membrane pressure of 400 kPa. The gas flow rates in the

permeate stream were measured by a bubble flow meter. The permeance of gas species *i*, P_i (mol $s^{-1}m^{-2}Pa^{-1}$) was calculated as per Eq. (1):

$$P_i = -\frac{J_i}{\Delta p} \qquad (1)$$

where J_i is the molar flux (mol $s^{-1}m^{-2}$) of gas species *i* and Δp is the transmembrane pressure difference (Pa). Permselectivity of species *i* over *j* ($\alpha_{i/j}$) was calculated as the ratio of permeances of the respective gases measured at the same temperature and pressure, as shown in Equation (2):

$$\alpha_{i/j} = \frac{P_i}{P_j} \qquad (2)$$

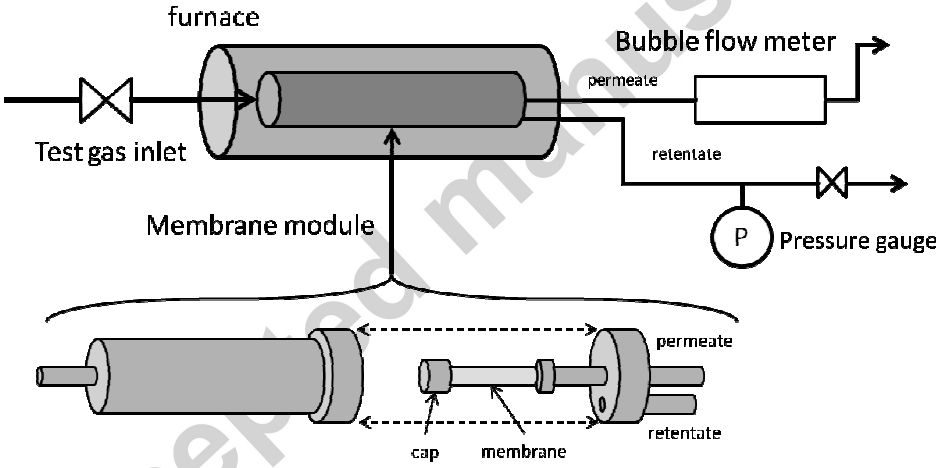

Fig. 1. Permeation setup

3 Results and discussion

Fig. 2A shows a representative nitrogen adsorption isotherm of all iron cobalt oxide silica xerogels. It shows a type I isotherm with a complete absence of hysteresis loop which exhibits a very strong initial adsorption at very low partial pressures ($P/P_o < 0.1$) followed by saturation, a characteristic of microporous materials. Figure 2B indicates that the incorporation of iron and cobalt oxides in different compositions did not present any significant difference in the structural parameters. The average BET surface areas for all xerogels were similar around 260 $m^2 g^{-1}$ (±16 $m^2 g^{-1}$) and likewise

pore volumes 0.134 $m^3 g^{-1}$ (±0.008 $m^3 g^{-1}$) and average pore sizes 20 Å (±1.5 Å), showing less than 10% variation. These results suggest that the pore structures of silica xerogels are generally independent from iron or cobalt oxide compositions.

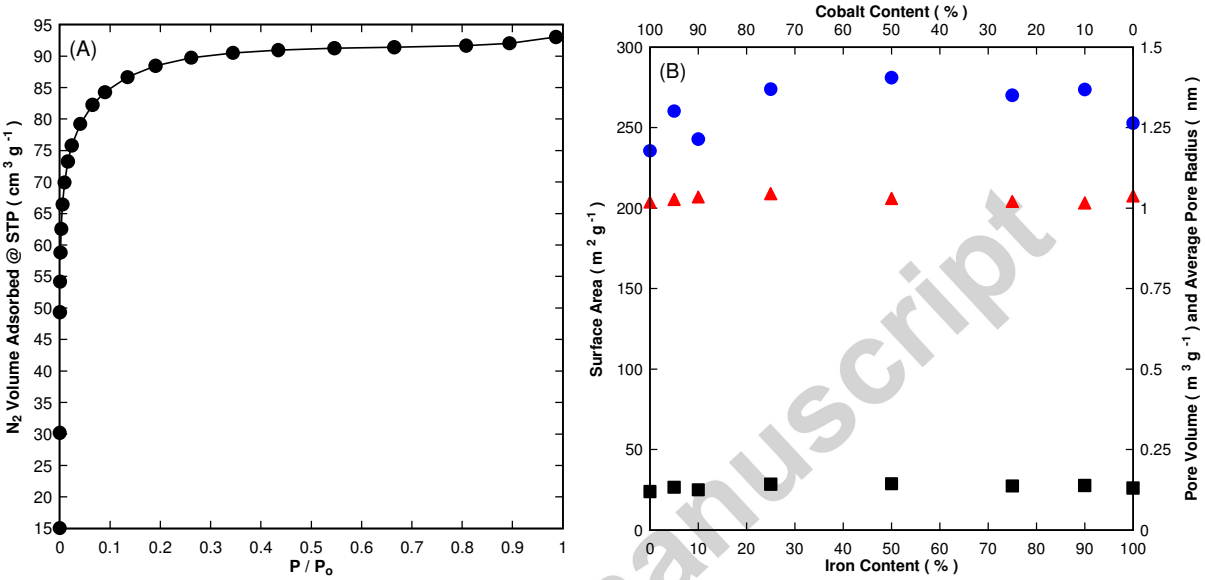

Fig. 2. (A) Typical N_2 adsorption isotherm and (B) surface area (■), pore volume (●) and average pore radius (▲) as a function of the Fe/Co silica xerogels calcined at 600 °C.

A representative FTIR spectrum is depicted in Fig. 3A. The peaks observed in the spectral regions around 1080 and 790 cm^{-1}, in addition to a shoulder at ~1200 cm^{-1}, are assigned to stretching vibrations in Si–O–Si (siloxane) bonds which are typical for silica xerogel materials. The shoulder at 960 cm^{-1} is assigned to vibration of the Si–OH (silanol) bonds [32, 33] whilst a small peak around 660 cm^{-1} is associated with Co_3O_4 [34-37]. The inset of Fig. 3A displays the spectral region between 600 and 530 cm^{-1}. This region shows low intensity peaks at 570 cm^{-1} for the Fe/Co 0/100 sample assigned to Co_3O_4 [34-37] and at 540 cm^{-1} for the Fe/Co 100/0 sample ascribed to Fe_2O_3 [38]. For the Fe/C0 50/50 silica xerogel, both low intensity peaks are also observed. To further understand the effect of iron and cobalt composition on silica matrices, the deconvoluted FTIR spectra of each xerogel was analysed with multiple Gaussian fitting functions. Fig. 3B shows the

ratio of the relative area of the peaks assigned to silanol bonds (centred ~960 cm^{-1}) and siloxane bonds (centred ~1080 cm^{-1}) as a function of the metal oxide composition. The results indicate that the addition of iron into the silica matrix decreases the number of silanol groups with respect to siloxane bridges. These results strongly suggest that iron oxide is favouring the condensation reactions in the binary iron cobalt silica sol-gel method, whilst cobalt oxide tends to inhibit the condensation reactions.

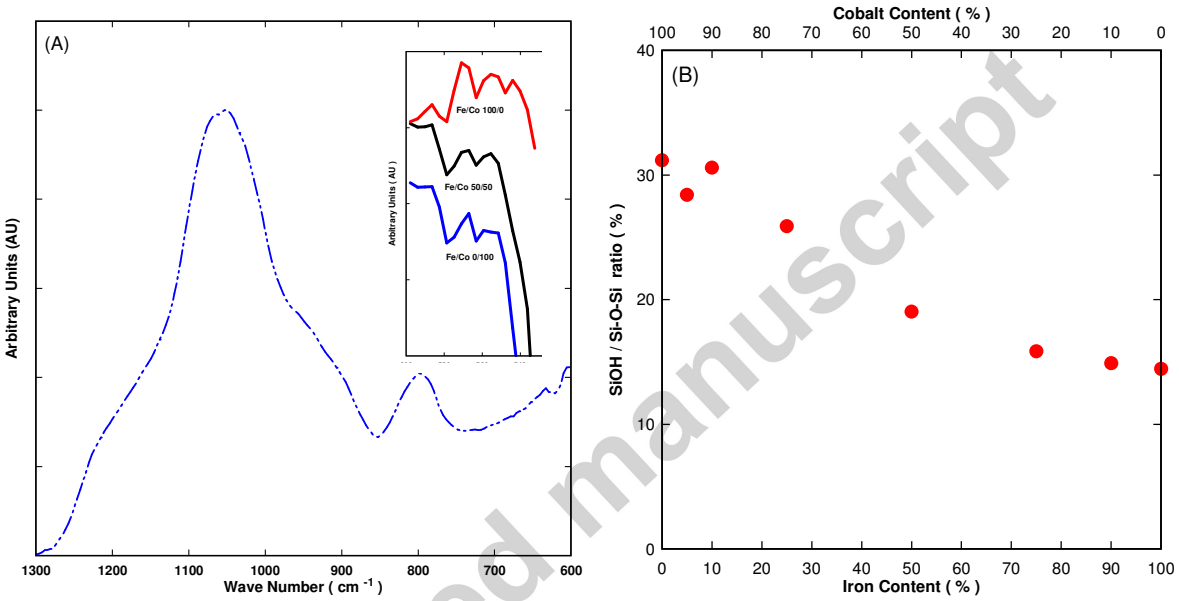

Fig. 3. (A) FTIR spectra of a Fe/Co 50/50 oxide silica xerogel and (B) evolution of the silanol to siloxane ratio (e.g. based on the ratio of FTIR peak areas) as a function of the Fe/Co composition. All samples were calcined at 600 °C.

Representative SEM micrographs along with the EDX mapping (for Si, Co, and Fe) of a Fe/Co=50/50 silica xerogels are illustrated in Fig. 4. Different colours are associated with diverse emission lines where each colour in the picture refers to the single emission energy of the element of interest. It can be seen that the iron oxide, cobalt oxide species and silica oxide species were generally well distributed (Figs. 4A-C). These results establish that the incorporation of iron and cobalt in silica xerogel was uniform throughout the entire xerogel surface. Further, a small number of large particles were observed (Fig. 4D). These correlate to the white spots in the circled area in

Fig. 4C, representing higher concentrations of cobalt. The EDX atom composition analysis results show that the Fe/Co ratio at these larger particles was 0.46. Therefore, the larger particles had the propensity to be dominated by cobalt oxide, though the tested xerogel had equimolar ratios of both cobalt and iron oxides.

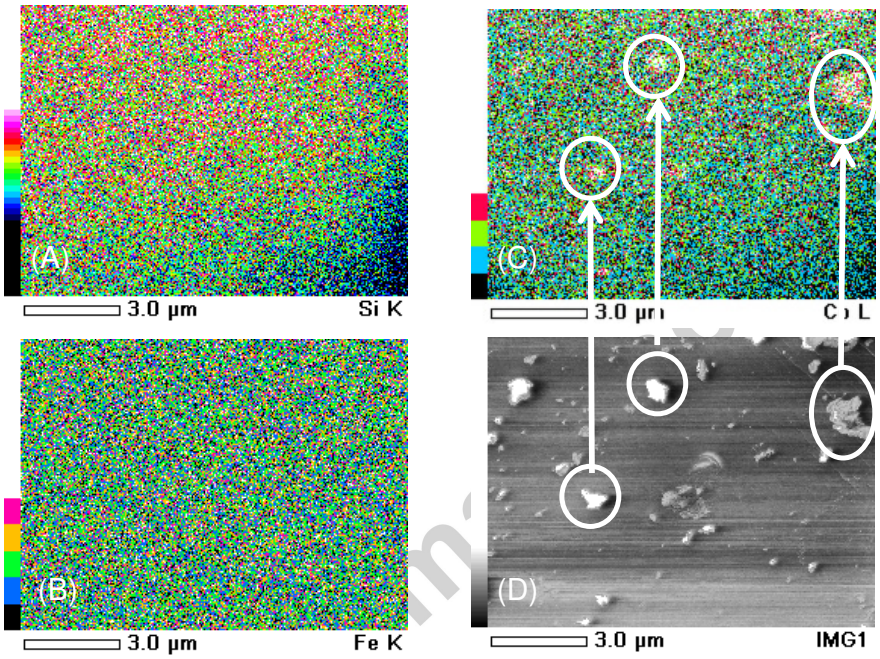

Fig. 4. SEM micrograph and EDX mapping of Fe/Co=50/50 iron cobalt oxide silica xerogel.

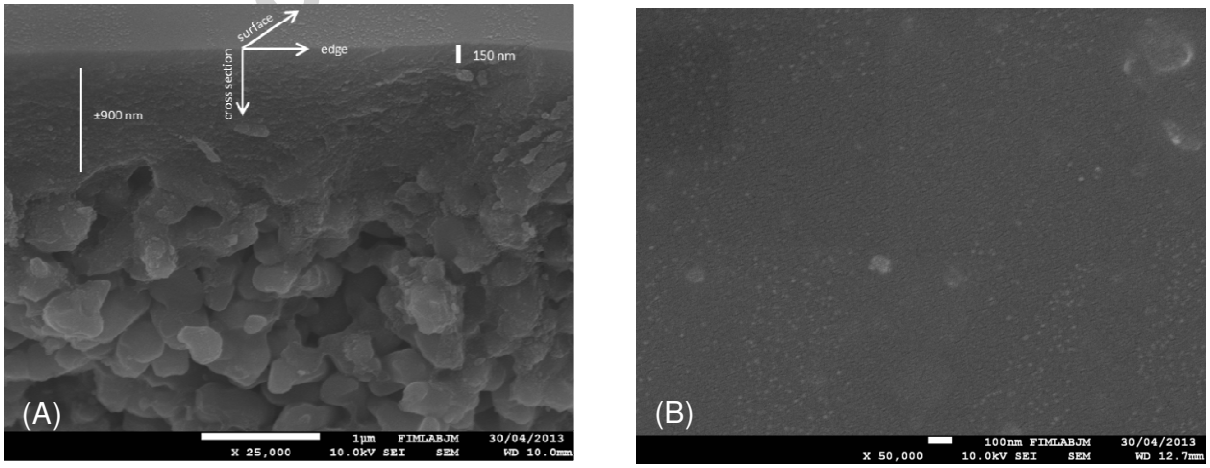

Fig. 5. SEM micrographs of Fe/Co=25/75 silica membrane at the (A) cross-section and (B) surface.

A representative SEM micrograph of a membrane cross-section is shown in Fig. 5A. The iron cobalt oxide silica top layer has a typical thickness of 150 nm which has a good uniformity with a clear boundary with the support γ-Al_2O_3 layer of 900 nm in thickness over the entire surface area of the membrane. The estimated membrane thickness also correlates well with previously published studies for cobalt silica membranes [20, 21]. A relatively smooth membrane surface is displayed in the top-layer (Fig. 5B), though a few large particles are observed on the surface similar to the xerogel micrograph in Fig. 4D. Nevertheless, these large particles are well incorporated in the top layer and show no micro-cracks or other defects. Further, silica membranes with Fe/Co > 50/50 generally failed with micro-cracks (not shown), thus confirming the silica to iron oxide detrimental effect caused by their thermal expansion mismatch discussed in the introduction section. Hence, the results shown hereinafter are for silica membranes containing Fe/Co molar ratios of 10, 25 and 50. Lower Fe/Co ratios below 10 were not considered to prepare membranes based on xerogel studies. For instance, in our previous work [24], Fe/Co=2 silica xerogels underwent a strong structural densification, whilst in this work the average pore radius (Fig. 2a) for the Fe/Co=10 was lower than Fe/Co=5. Therefore, these parameters indicate that Fe/Co=10 silica membrane may deliver a higher flux and permselectivity as compared to the silica membranes prepared with Fe/Co =2 or 5, respectively. As structural variations were very minor for Fe/Co molar ratios between 20 and 50 [24], then the preparation of membranes used an average value of Fe/Co=25, and two extreme cases of lower Fe/CO=10 and higher Fe/Co=50 values.

Fig. 6 shows that the permeance for all membranes increased for the smaller gases He (d_k = 2.6 Å) and H_2 (d_k = 2.89 Å) as a function of temperature, whilst decreasing or almost constant for larger gases, CO_2 (d_k = 3.3 Å) and N_2 (d_k = 3.64 Å). These results give a temperature dependent transport for gases with different molecular sizes, a characteristic of molecular sieving membranes. Close examination of the permeance results suggest that the Fe/Co ratio has produced different molecular

sieving structures. For instance, increasing the iron content led to an increase in the permeance of the larger gas molecules N_2 and CO_2. This can be clearly seen as the silica membranes containing Fe/Co at 10/90, 25/75 and 50/50, the permeance of these gases increased from ~ $2x10^{-8}$ to $7x10^{-8}$ and $2x10^{-7}$ at 500°C, respectively. Thus an order of magnitude increase occurred as the iron content increased from 10 to 50%.

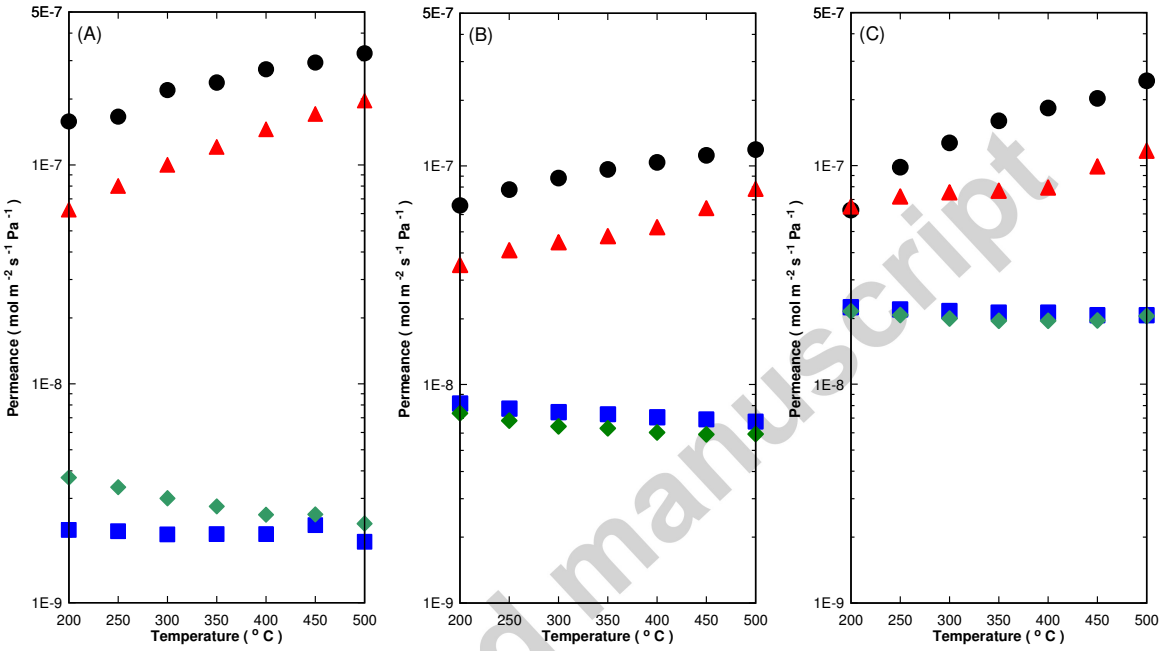

Fig. 6. Single gas permeation test for iron cobalt oxide silica membranes (A) Fe/Co = 10/90, (B) Fe/Co = 25/75, (C) Fe/Co = 50/50 for gases: He (●), H_2 (▲), N_2 (■) and CO_2 (◆).

The permeation behaviour of the iron cobalt oxide silica membranes is further highlighted by the gas permselectivities displayed in Fig. 7A. The Fe/Co=10/90 silica membrane delivered the best performance with He/N_2 permselectivities rising steeply as a function of temperature. For instance, best permselectivities were 170 (He/N_2) at 500 °C. In contrast, the Fe/Co=25/75 and Fe/Co=50/50 silica membranes achieve moderate He/N_2 permselectivities of 17.6 and 11.8, respectively. Figure 7B shows a pore size distribution of the membranes tested at 500 °C using gases with different kinetic diameters as molecular probes. The Fe/Co=10/90 silica membrane showed a very sharp drop of permeance between H_2 and CO_2 of almost two orders of magnitude. This clearly indicates that

the Fe/Co silica structure had constrictions between the kinetic diameters of H_2 and CO_2, with an average size in the region of 3Å. In contrast, the other two membranes resulted in smaller drop of permeances between these gases of 12.9 and 5.5 for the 25/75 and 50/50 Fe/Co silica membranes, respectively. These H_2/CO_2 permeselectivities are modest and just above the ideal Knudsen selectivity of 4.69. In order words, the membranes with the Fe content in excess of 10 mol% in the binary metal composition resulted in a broader pore size distribution than the membrane with Fe content equal to 10 mol%.

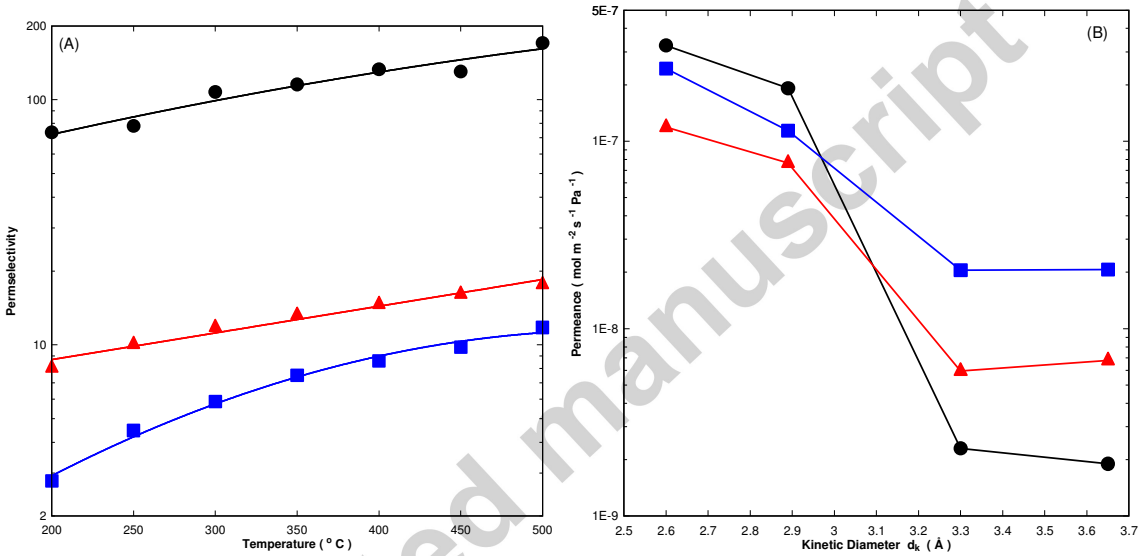

Figure 7. Silica membranes with Fe/Co molar ratios of 10/90 (●), 25/75 (▲) and 50/50 (■): (A) He/N_2 permselectivities and (B) pore size distribution based on permeance at 500 °C as a function of kinetic diameters for He (2.6Å), H_2 (2.89Å), CO_2 (3.3Å) and N_2 (3.64Å).

Single cobalt oxide silica membranes were also prepared to compare with the binary cobalt iron silica membrane. However, the single cobalt oxide silica membrane consistently delivered lower permselectivites for all gases as compared to the Fe/Co 10/90 silica membranes. For instance, He/N_2 values of 22.7 at 500 °C for the Fe/Co 0/100 were much lower than 170 for the Fe/Co 10/90 silica membrane, though comparable with the Fe/Co 25/75 and better than the Fe/Co 50/50 silica membranes. We are aware that single cobalt oxide silica membranes can reach permselectivities varying from ~ 10 at 100 °C to very high values close to 1000 at 500 °C for He/N_2, He/CO_2, H_2/N_2

and H_2/CO_2 [20]. Nevertheless and by taking into consideration the trade-off between fluxes and separation factors, the Fe/Co=10 silica membranes performed much better than the high quality pure Co oxide silica membrane at certain conditions. For instance, the fluxes for He and H_2 for the Fe/Co=10 silica membrane were almost one order of magnitude higher at 200 and 300 ^oC, whilst the permselectivities of 75 were slightly higher, by 10-20% at 200 ^oC, and similar at 300 ^oC. However, at higher temperatures (400 and 500 ^oC) the pure cobalt oxide silica membrane [20] showed superior performance. An additional point of importance is that the sol-gel method used in this work is slightly different from those published for cobalt oxide silica membranes. Due to the fact that mixing iron nitrates with peroxide causes excessive heat and possible explosion, contrary to cobalt nitrate and peroxide, the sol-gel preparation sequence in this work followed: (1) mix ethanol plus cobalt nitrate plus iron nitrate, (2) add peroxide, and (3) add TEOS. Conventionally, the sol-gel sequence is (1) mix cobalt nitrate with peroxide, (2) add ethanol, and (3) add TEOS [17-21]. Hence, dissolving metal nitrates on directly in peroxide has advantages in the structural pore size tailoring of doped silica membranes.

The binary metal oxide doping using iron and cobalt oxides at different ratios yielded different permeation and gas separation results. The nitrogen adsorption results showed that the structural variations in pore size and pore size distribution were not significant as a function of the Fe/Co molar ratio. However, these results differ from the gas permeation tests. In principle, gases with varying molecular sizes provide a superior molecular probing test in thin films rather than nitrogen adsorption in xerogels. Therefore, these results suggest that the combination of these metal oxides led to the formation of structures with different pore sizes, or at the very least different sized bottle necks or constrictions which ultimately control gas separation or selectivity. Hence, the interfacial structures between silica and the agglomerated iron cobalt oxide particles are playing an important role in molecular sieve structure formation. This point correlates well for the membranes with the best performance. For instance, the Fe/Co 10/90 silica membranes showed the highest silanol to

siloxane ratio. It is well known that superior pore size tailoring around 3-5 Å can be achieved by a high concentration of silanol groups [38]. In other words, cobalt oxide tends to inhibit the condensation reactions thus favouring hydrolysis reactions. Contrary to this trend, increasing the content of iron oxides led to an increase of the condensed species (i.e. siloxane bridges) and a reduction in the separation capabilities of the membranes. Nevertheless the binary Fe/Co doping of silica membranes provided superior pore size tailorability than Pd/Co, as the best He/N_2 selectivities of 170 in this work are higher than 70 [30], respectively, equivalent to an improvement of 143%.

4 Conclusions

It was found that iron and cobalt oxide particles dispersed quite well in the silica matrix, though minor patches of rich in cobalt oxide were observed. All Fe/Co oxide silica membranes delivered activated transport, a characteristic of molecular sieving structures, as the permeance of the smaller gas molecules (He and H_2) increased with temperature, whilst the larger gas molecules (CO_2 and N_2) decreased or remained almost constant. The Fe/Co ratio altered the chemical structure of the resultant silica functional groups. A higher content of iron oxide increased the condensation reaction, thus forming more siloxane bridges which in principle tend to increase the pore size of silica materials. As a result, the separation capability of membranes with high iron content decreased delivering modest performance. On the contrary, increasing the cobalt content inhibited the condensation reactions, leading to higher silanol to siloxane ratios. In this case, superior molecular sieving structures were formed, with average pore sizes in the region of 3Å. Therefore, the permeance of the large gas molecules decreased by up to one order of magnitude for the higher cobalt content membranes as compared with higher iron content, and gas permselectivities increased significantly, up to 170 for He/N_2 at high temperatures of 500 °C.

Acknowledgement

The authors acknowledge funding support from the Australian Research Council (ARC) Discovery Program (DP110101185). J. C. Diniz da Costa gratefully thanks the support given by the ARC Future Fellowship Program (FT130100405).

References

[1] M. Kanezashi, M. Asaeda, Hydrogen permeation characteristics and stability of Ni-doped silica membranes in steam at high temperature, J. Memb. Sci., 271 (2006) 86-93.

[2] M. Kanezashi, T. Fujita, M. Asaeda, Nickel-doped silica membranes for separation of helium from organic gas mixtures, Sep. Sci. Technol., 40 (2005) 225-238.

[3] D. Uhlmann, S. Smart, J.C. Diniz da Costa, High temperature steam investigation of cobalt oxide silica membranes for gas separation, Sep. Purif. Technol., 76 (2010) 171-178.

[4] M. Kanezashi, D. Fuchigami, T. Yoshioka, T. Tsuru, Control of Pd dispersion in sol–gel-derived amorphous silica membranes for hydrogen separation at high temperatures, J. Memb. Sci., 439 (2013) 78-86.

[5] T. Tsuru, S.I. Wada, S. Izumi, M. Asaeda, Silica-zirconia membranes for nanofiltration, J. Memb. Sci., 149 (1998) 127-135.

[6] K. Yoshida, Y. Hirano, H. Fujii, T. Tsuru, M. Asaeda, Hydrothermal stability and performance of silica-zirconia membranes for hydrogen separation in hydrothermal conditions, J. Chem. Eng. Jpn., 34 (2001) 523-530.

[7] D. Uhlmann, S. Liu, B. P. Ladewig, J. C. Diniz da Costa, Cobalt-Doped Silica Membranes for Gas Separation, J. Memb. Sci., 326 (2009) 316–321.

[8] Y. Gu, S.T. Oyama, Permeation properties and hydrothermal stability of silica-titania membranes supported on porous alumina substrates, J. Memb. Sci., 345 (2009) 267-275.

[9] V. Boffa, D.H.A. Blank, J.E. ten Elshof, Hydrothermal stability of microporous silica and niobia-silica membranes, J. Memb. Sci., 319 (2008) 256-263.

[10] H. Qi, H. Chen, L. Li, G. Zhu, N. Xu, Effect of Nb content on hydrothermal stability of a novel ethylene-bridged silsesquioxane molecular sieving membrane for H_2/CO_2 separation, J. Memb. Sci., 421–422 (2012) 190-200.

[11] G.P. Fotou, Y.S. Lin, S.E. Pratsinis, Hydrothermal stability of pure and modified microporous silica membranes, J. Memb. Sci., 30 (1995) 2803-2808.

[12] J.H. Lee, S.C. Choi, D.S. Bae, K.S. Han, Synthesis and microstructure of silica-doped alumina composite membrane by sol-gel process, J. Mater. Sci. Letters, 18 (1999) 1367-1369.

[13] R. Igi, T. Yoshioka, Y.H. Ikuhara, Y. Iwamoto, T. Tsuru, Characterization of co-doped silica for improved hydrothermal stability and application to hydrogen separation membranes at high temperatures, J. Am. Ceram. Soc., 91 (2008) 2975-2981.

[14] S. Battersby, S. Smart, B. Ladewig, S. Liu, M.C. Duke, V. Rudolph, J.C. Diniz da Costa, Hydrothermal stability of cobalt silica membranes in a water gas shift membrane reactor, Sep. Purif. Technol., 66 (2009) 299-305.

[15] K. Yoshida, Y.H. Ikuhara, S. Takahashi, T. Hirayama, T. Saito, S. Sueda, N. Tanaka, P.L. Gai, The three-dimensional morphology of nickel nanodots in amorphous silica and their role in high-temperature permselectivity for hydrogen separation, Nanotechnology, 20 (2009) 315703.

[16] Y.H. Ikuhara, H. Mori, T. Saito, Y. Iwamoto, High-temperature hydrogen adsorption properties of precursor-derived nickel nanoparticle-dispersed amorphous silica, J. Am. Ceram. Soc., 90 (2007) 546-552.

[17] G. Olguin, C. Yacou, S. Smart, J.C. Diniz da Costa, Tailoring the oxidation state of cobalt through halide functionality in sol-gel silica, Scientific Reports, 3 (2013) 2449.

[18] C.R. Miller, D.K. Wang, S. Smart, J.C. Diniz da Costa, Reversible redox effect on gas permeation of cobalt doped ethoxy polysiloxane (ES40) membranes, Scientific Reports, 3 (2013) 1648.

[19] D. Uhlmann, S. Smart, J.C. Diniz da Costa, H_2S stability and separation performance of cobalt oxide silica membranes, J. Memb. Sci., 380 (2011) 48-54.

[20] C. Yacou, S. Smart, J.C. Diniz da Costa, Long term performance cobalt oxide silica membrane module for high temperature H_2 separation, Energy Environ. Sci., 5 (2012) 5820-5832.

[21] S. Smart, J.F. Vente, J.C. Diniz da Costa, High temperature H_2/CO_2 separation using cobalt oxide silica membranes, Int. J. Hydrogen Energy, 37 (2012) 12700-12707.

[22] D.K. Wang, J.C. Diniz da Costa, S. Smart, Development of rapid thermal processing of tubular cobalt oxide silica membranes for gas separations, J. Memb. Sci., 456 (2014) 192-201.

[23] D.K. Wang, J. Motuzas, J.C. Diniz da Costa, S. Smart, Rapid thermal processing of tubular cobalt oxide silica membranes, Int. J. Hydrogen Energy, 38 (2013) 7394-7399.

[24] A. Darmawan, S. Smart, A. Julbe, J.C. Diniz da Costa, Iron Oxide Silica Derived from Sol-Gel Synthesis, Materials, 4 (2011) 448-456.

[25] I. Šimkienė, M. Treideris, G. Niaura, R. Szymczak, P. Aleshkevych, A. Rėza, I. Kašalynas, V. Bukauskas, G.J. Babonas, Multifunctional iron and iron oxide nanoparticles in silica, Mater. Chem. Phys., 130 (2011) 1026-1032.

[26] M.D. Alcalá, C. Real, Synthesis based on the wet impregnation method and characterization of iron and iron oxide-silica nanocomposites, Solid State Ionics, 177 (2006) 955-960.

[27] C. Chaneac, E. Tronc, J.P. Jolivet, Magnetic iron oxide-silica nanocomposites. Synthesis and characterization, J. Mater. Chem., 6 (1996) 1905-1911.

[28] S.G. Marchetti, M.V. Cagnoli, A.M. Alvarez, N.G. Gallegos, J.F. Bengoa, A.A. Yeramian, R.C. Mercader, Dependence of the oxide-support interaction on the size and nature of iron oxide particles on SiO_2, J. Phys. Chem. Solids, 58 (1997) 2119-2125.

[29] M. Takeda, T. Onishi, S. Nakakubo, S. Fujmoto, hysical Properties of Iron-Oxide Scales on Si-Containing Steels at High Temperature, Mater. Transac., 50 (2009) 2242-2246.

[30] B. Ballinger, J. Motuzas, S. Smart, J.C. Diniz da Costa, Palladium cobalt binary doping of molecular sieving silica membranes, J. Memb. Sci., 451 (2014) 185-191.

[31] B. S. Bonekamp, A. van Horssen, L. A. Correia, J. F. Vente, W. G. Haije, Macroporous support coatings for molecular separation membranes having a minimum defect density. J. Membr. Sci., 278 (2006) 349-56.

[32] A. Bertoluzza, C. Fagnano, M. Antonietta Morelli, V. Gottardi, M. Guglielmi, Raman and infrared spectra on silica gel evolving toward glass, J. Non-Crystal. Solids, 48 (1982) 117-128.

[33] A. Duran, C. Serna, V. Fornes, J.M. Fernandez Navarro, Structural considerations about SiO2 glasses prepared by sol-gel, J. Non-Crystal. Solids, 82 (1986) 69-77.

[34] A.Y. Khodakov, J. Lynch, D. Bazin, B. Rebours, N. Zanier, B. Moisson, P. Chaumette, Reducibility of Cobalt Species in Silica-Supported Fischer-Tropsch Catalysts, J. Catalys., 168 (1997) 16-25.

[35] B. Pejova, A. Isahi, M. Najdoski, I. Grozdanov, Fabrication and characterization of nanocrystalline cobalt oxide thin films, Mater. Res. Bul., 36 (2001) 161-170.

[36] C.-W. Tang, C.-B. Wang, S.-H. Chien, Characterization of cobalt oxides studied by FT-IR, Raman, TPR and TG-MS, Thermochimica Acta, 473 (2008) 68-73.

[37] G.A. Santos, C.M.B. Santos, S.W. da Silva, E.A. Urquieta-González, P.P.C. Sartoratto, Sol–gel synthesis of silica–cobalt composites by employing Co_3O_4 colloidal dispersions, Coll. Surf. A: Physicochemical and Eng. Asp., 395 (2012) 217-224.

[38] N. Du, Y. Xu, H. Zhang, C. Zhai, D. Yang, Selective Synthesis of Fe_2O_3 and Fe_3O_4 Nanowires Via a Single Precursor: A General Method for Metal Oxide Nanowires, Nanoscale Res. Letters, 5 (2010) 1295 - 1300.

[39] C.J. Brinker, R. Sehgal, S.L. Hietala, R. Deshpande, D.M. Smith, D. Loy, C.S. Ashley, Sol-gel strategies for controlled porosity inorganic materials, J. Memb. Sci., 94 (1994) 85-102.

Research Highlights

- Binary iron cobalt silica membrane prepared via sol-gel method.
- Fe content favoured condensation reactions and siloxane bridges.
- Co content inhibited condensation and favoured the formation of silanols.
- Best performance for silica membranes with low Fe and high Co content.

Graphical Abstract